Comparison of Force-Based and Displacement-Based seismic design of dissipative post-tensioned rocking timber wall systems

F. Sarti, A. Palermo & S. Pampanin

Civil and Natural Resource Engineering Department, University of Canterbury, Christchurch, New Zealand

2015 NZSEE Conference

ABSTRACT: Based on numerical studies performed by the authors, the paper presents to Force-Based (FBD) and Displacement-Based (DBD) seismic Design provisions for dissipative post-tensioned rocking timber wall (Pres-Lam) systems.

At first, a discussion on the seismic design requirements of post-tensioned rocking timber wall systems is provided, including suggested material limit states to be considered in the design phase (Ultimate Limit State) also aimed to prevent collapse in case of more severe events.

The required amendments to a Force-Based Design provision in accordance to NZS1170.5 are then discussed focussing on the development and significance of the inelastic spectrum scaling factor (k_μ).

Similarly, the key modifications to design equations required within a Displacement Based Design Provisions are proposed, based on extensive numerical analyses and focusing on the as the design inelastic displacement shape and the equivalent viscous damping.

In the final part of the paper a multi-storey building is designed using both FBD and DBD and the two different approaches are discussed.

1 INTRODUCTION

Dissipative post-tensioned rocking timber (Pres-Lam) wall systems are low-damage seismic-resistant elements which provide a combination of re-centering and dissipation.

Un-bonded post-tensioning reinforcement (either bars or strands) re-centers the system, while several devices can be used to provide energy dissipation. In walls systems, a first layout option is to concentrate the dissipative reinforcement at the base connection of the wall. Generally this configuration has either internal or external (replaceable) tension-compression yield mild steel dissipaters.

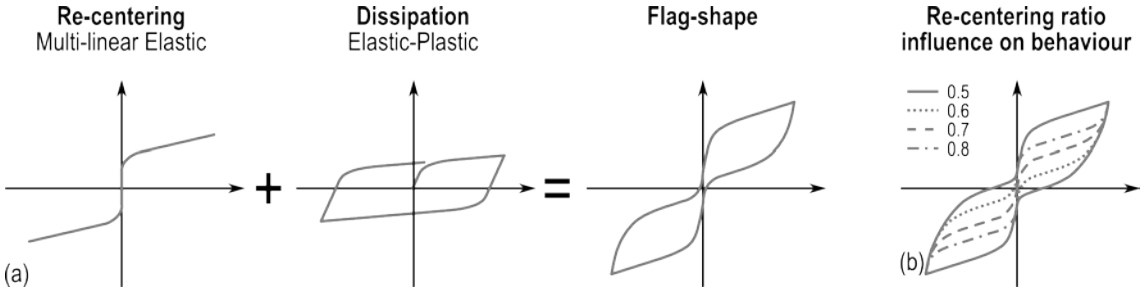

Figure 1. Qualitative moment-rotation behaviour of post-tensioned rocking connections. (a) re-centering and dissipative contributions to form a flag-shape and (b) influence of re-centering ratio.

The qualitative behaviour of a post-tensioned connection can be represented by the combination of a multi-linear elastic and a bi-linear hysteresis as shown in Figure 1a. The combination of the two hysteretic rules generates the "flag-shape" hysteresis. The shape of this relationship is governed by the re-centering ratio, β, defined as the ratio of the post-tensioning and total moment contributions ($\beta = M_{pt}/M_{tot}$)

Figure 1 qualitatively shows the influence of this parameter on the hysteric behaviour of the connection. For the unit value of β, the connection behaves following a multi-linear elastic (post-tensioned only) relationship, with no hysteretic dissipation; instead, for $\beta = 0$ the connection is a mild steel only option with plenty of hysteretic dissipation and significant residual displacement. A minimum value of 0.6 is suggested, ensuring acceptable levels of dissipation and negligible residual displacements.

The structural system was originally developed and tested for precast concrete application during the PREstress Seismic Structural Systems (PRESSS) program in the 1990s (Priestley 1991; Priestley et al. 1999) and more recently extended to structural steel (Christopoulos et al. 2002) and engineered wood elements (Palermo et al. 2005; Smith et al. 2007; Newcombe et al. 2008; Newcombe et al. 2010b; Newcombe et al. 2010a; STIC 2013).

The paper first discusses the performance-based design approach of dissipative post-tensioned timber walls with detailed discussion on material limit state to be adopted in the section design also aimed to prevent collapse under more severe events.

The key modifications required to Force-Based and Displacement-Based Design approaches are summarized, and based on extensive numerical analyses in accordance to the FEMA P-695 procedure (ATC, 2009) used in the last part of the paper which provide a comparison and discussion on the results of the two design approaches.

2 PERFORMANCE-BASED DESIGN PHILOSOPHY

The general performance-based design philosophy of post-tensioned timber systems can be qualitatively summarized by Figure 2. The general0020hierarchy of strength and sequence of events recommended for these systems (STIC, 2013) would be: (i) Yielding of the non-prestressed reinforcement (or dissipaters); (ii) Yielding of the timber at the rocking interface either in the column or the beam; and finally (iii) Yielding of the post-tensioning reinforcement.

Such design philosophy allows the system to (i) withstand small and frequent events with no significant damage; (ii) provide the required hysteretic damping under a design level earthquake; (iii) prevent structural collapse when subjected to a Maximum Considered Event (MCE).

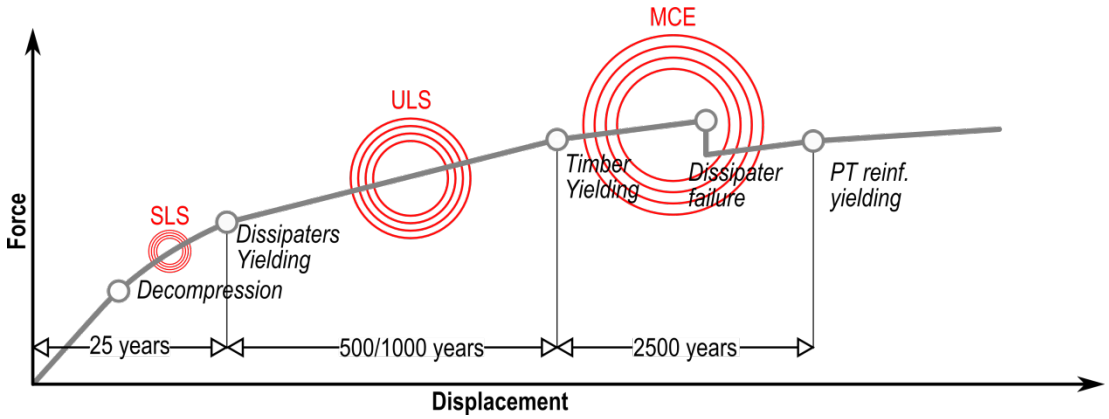

Figure 2. Qualitative push-over curve and performance limits.

The proposed system design requirements include suggested values of re-centering ratio, strain limits in the dissipaters at Design Base Event (DBE) and Maximum Considered Event (MCE) level and initial timber stress:

- Initial timber stress should not exceed 10% of the timber compressive strength. This stress limit is set to allow the section to develop the gap opening and neutral axis depth necessary to the efficient activation of the dissipaters.
- The maximum strain in the tension-compression yield dissipaters shall be in the range of 3-4% at DBE level and 6% at MCE level (Sarti et al. 2013). The strain range suggested allows the system to develop the necessary damping while providing the dissipater with some failure margin.
- Values of re-centering ratio (β) at design level should not be less than 0.6 (60% re-centering contribution and 40% dissipative contribution).

3 ANALYSIS METHODOLOGY

The numerical analyses carried out to support the calibration of the seismic design provisions in accordance to either a Force-Based was carried out following the FEMA P-695 procedure. The procedure utilizes nonlinear analysis techniques, and explicitly considers uncertainties in ground motion, modelling, design, and test data. The technical approach is a combination of traditional code concepts, advanced nonlinear dynamic analyses, and risk-based assessment techniques (ATC 2009).

The final aim of the procedure is to determine significant FBD design parameters in accordance to ASCE/SEI 7-10 (ASCE/SEI, 2010) such as the seismic modification factor (R), over-strength factor (Ω_0) and deflection amplification factor (C_d). For brevity, the most significant aspects of the numerical methodology are discussed in the paper and further information can be found in ATC (2009) and Sarti et al. (2014b).

The numerical methodology with minor modifications was also used to determine significant Displacement-Based Design procedure parameters.

3.1 Case study buildings

The basic plan view configuration of the archetype buildings is shown in Figure 3. The building has an approximate plan of 32m (4 bays) in the longitudinal direction and 18m (3 bays) in the transverse direction with a floor area of approximately 600m^2 per floor. The standard building configuration has post-tensioned timber walls providing lateral load resistance in both the longitudinal and the transversal direction (STIC 2013). Five three-bay frames spanning 6m in the transverse direction support gravity loads.

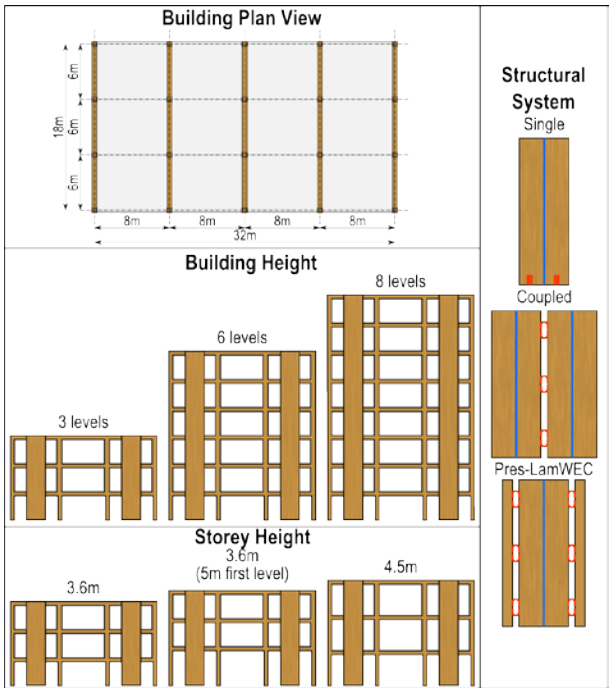

Figure 3.Case study buildings parameters.

Table 1. Case study buildings summary.

ID	No. of storeys	H_1	H	Wall depth	Floor system	Storey mass
		(m)	*(m)*	*(m)*		*(t)*
1	3	3.6	3.6	3.6	TCC	320
2	3	4.5	4.5	3.6	TCC	320
3	6	3.6	3.6	4.8	TCC	320
4	6	5	3.6	4.8	TCC	320
5	6	4.5	4.5	4.8	TCC	320
6	8	3.6	3.6	4.8	TCC	320
7	8	4.5	4.5	4.8	TCC	320
8	8	5	3.6	4.8	TCC	320
9	3	3.6	3.6	3.6	CLT	222
10	3	4.5	4.5	3.6	CLT	222
11	6	3.6	3.6	4.8	CLT	222
12	6	5	3.6	4.8	CLT	222
13	6	4.5	4.5	4.8	CLT	222
14	8	3.6	3.6	4.8	CLT	222
15	8	4.5	4.5	4.8	CLT	222
16	8	5	3.6	4.8	CLT	222

NOTE: TCC = Timber-Concrete Composite floor system, CLT = solid cross-laminated timber floor system.
H_1, H = first and upper levels inter-storey height.

Several parameters affecting the structural behaviour of the case study building were accounted for. Those included the building and inter-storey height, wall depth, gravity load magnitude as summarized in Figure 3 and Table 1.

For each case study building a different seismic resisting wall system was also considered, namely single walls, Column-wall-column and coupled wall systems.

3.2 **Model development**

The case study buildings were modelled using the model shown in Figure 4. The model uses a multi-spring element at the wall-foundation interface to simulate the gap opening. The modelling approach was first introduced by Spieth et al. (2004) for modelling post-tensioned rocking concrete systems, but the approach can be extended to timber systems as well (Newcombe, 2012; Smith, 2014).

To incorporate the P-Delta effects in OpenSEES (McKenna 2011), an additional column (i.e. P-delta column) was used. The P-Delta column was defined as an elastic beam-column element, with high axial stiffness and near-zero flexural stiffness. The storey nodes were subjected to a constant vertical force equal to the storey seismic weight.

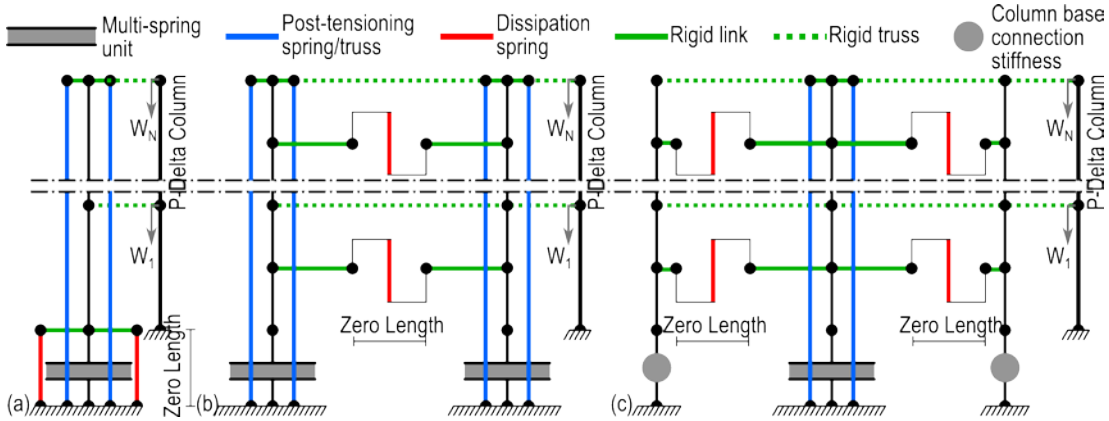

Figure 4. Multi-spring model.(a) Single wall model and material details. (b) Column-wall-column model. (c) Coupled walls model.

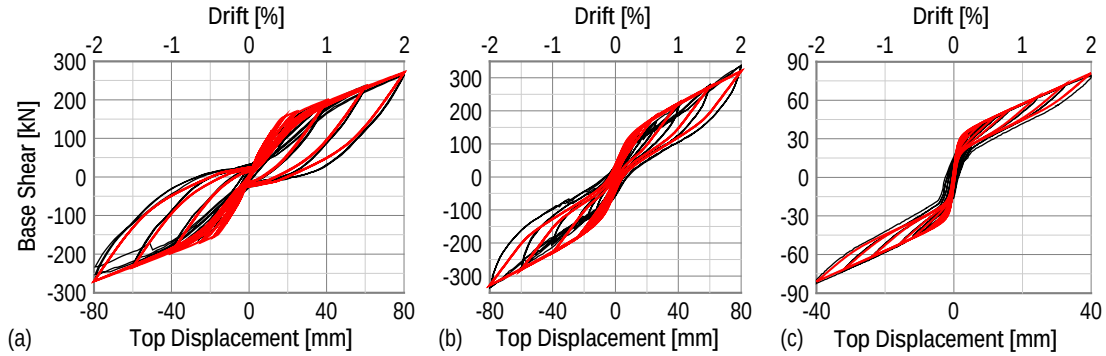

Figure 5. Numerical-experimental results comparison. (a) Single wall. (b) Pres-lamWEC system; (c) Couple walls.

The numerical model were calibrated and compared to available experimental data. In particular, experimental data by Sarti et al. (2014a) was used to calibrate the models for single walls and Pres-LamWEC system as shown in Figure 5a,b. Quasi-static cyclic tests by Iqbal et al. (2007) provided the calibration data for coupled walls systems (Figure 5c). As the results in Figure 5 show, the numerical model is capable of closely match the observed experimental results.

4 CALIBRATION OF FORCE-BASED DESIGN PARAMETERS

4.1 Reduction Factors

As part of the determination of the seismic performance factors an extensive numerical study was carried out by the authors (Sarti et al. 2014b) in accordance to the FEMA P-695 methodology (ATC, 2009). The objective of such methodology was the determination of the seismic performance factors in term of the seismic modification factor (R) and over-strength factors (Ω_0). While more details on the numerical work can be found in Sarti et al. (2014b), the paper focuses on a brief discussion on the extension of those numerical results to be applied to different standards.

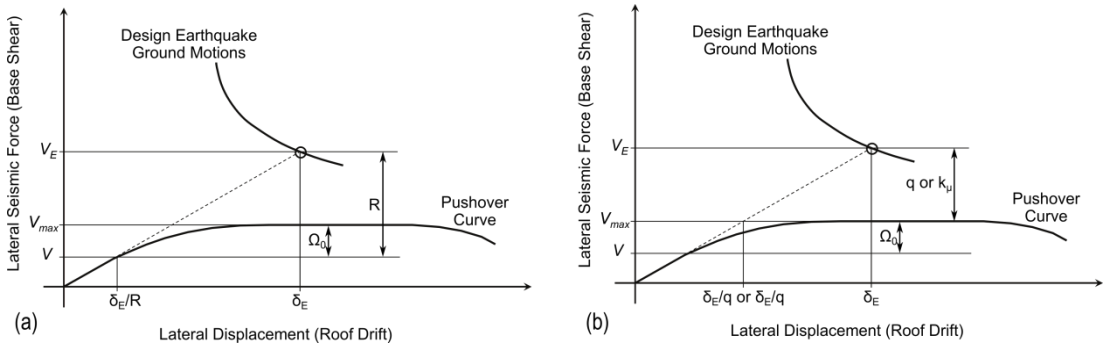

Figure 6. Definition of the seismic reduction factors in accordance to (a) ASCE 7-10 and (b) EC8 or NZS1170.5.

The main difference in the seismic design methodology is in the definition of the design point. As shown in Figure 6a seismic design in accordance to ASCE 7-10 (ASCE/SEI, 2010) requires that the ductile seismic resisting system is designed elastically for the reduced forces at yielding point. On the other hand, the design point of the lateral resisting system in accordance to NZS1170.5 (2004) or EC8 (European Committee for Standardization, 2004) is designed to fulfil some ductility and the equivalent elastic-perfectly plastic approximation is secant to the ULS demand rather than the yield point.

Therefore, the seismic reduction factor, R = 7, determined in the numerical study by Sarti et al. (2014b) can be modified to account for this different design approach giving either the suggested behaviour factor (EC8), q, or the inelastic spectrum scaling factor (NZS 1170.5), k_μ, as defined by Equation (1):

$$q, k_\mu = \frac{R}{\Omega_0} \tag{1}$$

Although a system over-strength factor of 3.5 may be adopted for the system as defined above and in accordance to the FEMA P-695 procedure, a quite significant variation in the over-strength factor for the different systems was observed; therefore, the average value across the different systems was adopted in the definition of a seismic reduction factor in accordance to other standards. As shown in Sarti et al. (2014b), the system over-strength factors were respectively 2.5, 3.0 and 3.5 for single wall, Pres-LamWEC and coupled walls systems and the average value across the different systems was approximately 3.0. As a result, seismic reduction factors of Equation (2) can be adopted:

$$q, k_\mu = \frac{R}{\Omega_0} = \frac{7.0}{2.97} = 2.36 \rightarrow 2.5 \tag{2}$$

4.2 **Estimation of natural period**

Another key point in the seismic force-based design of a multi-storey building is the estimation of the natural (or design) period of vibration.

Usually the coefficients of empirical formulas are calibrated for traditional steel or concrete structures and the estimation of the initial period was done by considering “other structures” type of coefficients. From a comparison of the numerical results this assumption was deemed over-conservative and different coefficients were used. In particular, among the coefficients reported in the standards, those showing a better fit to the numerical results were the ones related to moment-resisting concrete frames.

Figure 7a shows that the moment-resisting concrete frames empirical formulas provide a better estimation of the period of the structure up to 1.5s, while for higher periods the values were still under-estimated.

The Rayleigh method provided a better and more reliable estimation of the natural period, yet a modification shall be applied. The elastic stiffness of a seismic resisting system shall be defined as the secant-to-yield stiffness (representing the equivalent elastic-plastic system) rather than the “initial”. Adopting the initial flexural stiffness would again result in an under-estimation of the natural period of vibration of the structure.

Unlike concrete structures, the yield point of a post-tensioned rocking system is not of easy evaluation from a preliminary design point of view; therefore, it is suggested to evaluate the period considering the stiffness at decompression point and apply a magnification factor of 1.4, proposed in this section based on numerical results.

$$T_1 = 1.4 \cdot 2\pi \sqrt{\frac{\sum_{i=1}^{n} W_i d_i^2}{g \sum_{i=1}^{n} F_i d_i}} \tag{3}$$

Where d_i is the horizontal displacement of the center of mass at level *i*, F_i the displacing force acting at level *i*, i the level under consideration of structure, n number of levels in a structure, W_i the seismic weight at level *i*

The chart in Figure 7b reports the comparison of the numerical values against the value evaluated from Equation (3).

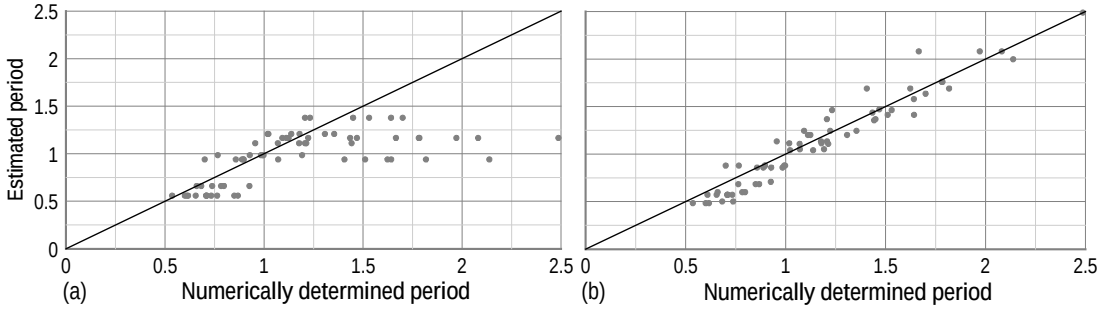

Figure 7. Natural period of vibration estimation methods. (a) Empirical method (2004); (b) modified Rayleigh method.

5 CALIBRATION OF DISPLACEMENT-BASED DESIGN PARAMETERS

The calibration of the Displacement-Based Design (Priestley *et al.*, 2007) parameters focussed on the determination of modification factors for the area-based hysteretic viscous damping and the inelastic displacement profile.

The former, was determined through quasi-static numerical analysis based on experimental data on single wall systems by Sarti et al. (2014a) and discussed in Section 5.1 below. The model shown in Section 3.2 was used.

The calibration of the design inelastic displacement profile was carried out through non-linear time-history analysis adopting the methodology described above.

5.1 Area-Based hysteretic viscous damping

As highlighted in single dissipative post-tensioned timber wall experimental tests (Sarti et al. 2014a), the area-based hysteretic damping was strongly influenced by the ratcheting behaviour of the dissipater as well as the dissipater connection flexibility (see Figure 1b).

Those effects were implemented in the multi-spring numerical model and quasi-static analyses were carried out with the variation of several design parameters. The analysis considered a set of case study walls with different cross-sectional dimensions (0.24m×2.4m and 0.36m×3.6m) and three elements heights (3, 6 and 8 storeys, 3m inter-storey height) were accounted for. To assess the influence of different re-centering ratios, each wall was designed using values of 0.6, 0.7 and 0.8.

Different dissipater connection stiffness values were considered as relative connection-dissipater stiffness factor.

The modification factor, k_ξ, was evaluated with Equation (1):

$$k_\xi = \frac{\xi_{numerical}}{\xi_{analytical}};\ \xi_{numerical} = \frac{1}{2\pi}\frac{A_h}{F_m\Delta_m};\ \xi_{analytical} = \frac{(2-2\beta)(\mu-1)}{\mu\pi\left[1+r(\mu-1)\right]} \quad (1)$$

Where $\xi_{numerical}$ is the numerical area-based hysteretic damping, A_h the area within one complete cycle of stabilized force-displacement response, F_m, Δ_m the maximum force and displacement achieved in the stabilized loops, $\xi_{numerical}$ the idealized flag-shaped hysteretic damping analytical formula (Priestley et al. 2007), μ the ductility, β the re-centering ratio and r the post-yield stiffness factor.

Figure 1a shows an example comparison between the analytical results and the numerical evaluated data.

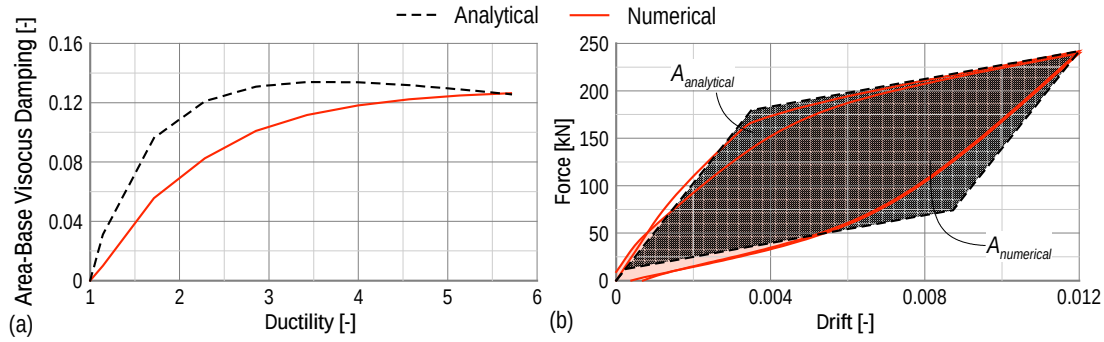

Figure 1. (a) Comparison of hysteretic damping evaluated from analytical and numerical data of a typical wall base connection; (b) Evaluation of hysteretic areas.

Figure 2 shows a summary of the numerical results which were fitted using linear functions reported in Equation (2).

$$k_{\xi} = 0.83 + (\mu - 1) \cdot \begin{cases} 0.06 \;\; w/\; isot.\; strain\, hard. \\ 0.02 \;\; w/o \;\; isot.\; strain\, hard. \end{cases} \tag{2}$$

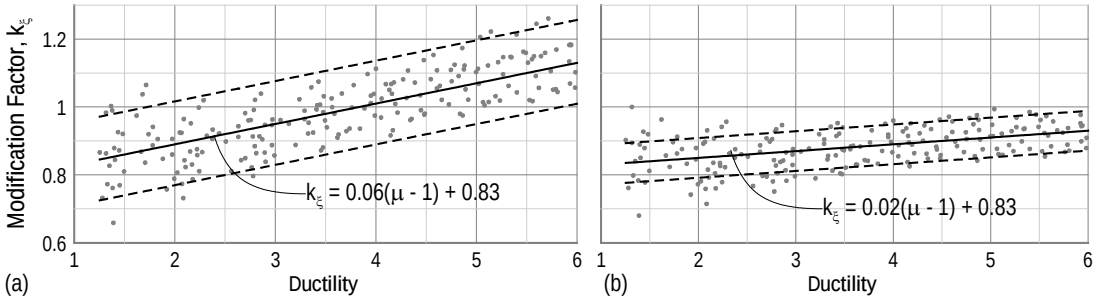

Figure 2. EVD modification factors (a) with and (b) without isotropic strain hardening effects.

Figure 2 and Equation (2) consider the isotropic strain hardening effect of the steel material. This distinction was necessary in order to properly account for the dissimilar behaviour of different devices. In fact, dissipater such as tension-compression yield device display significant isotropic strain hardening in compression (Sarti et al., 2013), while U-shaped Flexural Plates (UFPs) usually do not show any compressive yield shift (Skinner et al., 1974).

5.2 **Displacement profiles and inter-storey drift**

The case study buildings were designed in accordance to a DBD approach (Priestley *et al.*, 2007) using the above modification factors for the hysteretic viscous damping evaluation and the following design parameters: (a) Design drift θ_d = 1.2%; (b) ductility factor μ = 2.5; (c) post-yielding stiffness factor r = 0.2.

It is to be clarified that a linear displacement distribution was assumed in the design phase and was later compared to observed results.

The black plots in Figure 3 show the averaged peak displacement and inter-storey drift profiles resulting from extensive NLTHA. The results highlight that a linear profile was not appropriate for buildings taller than three storeys.

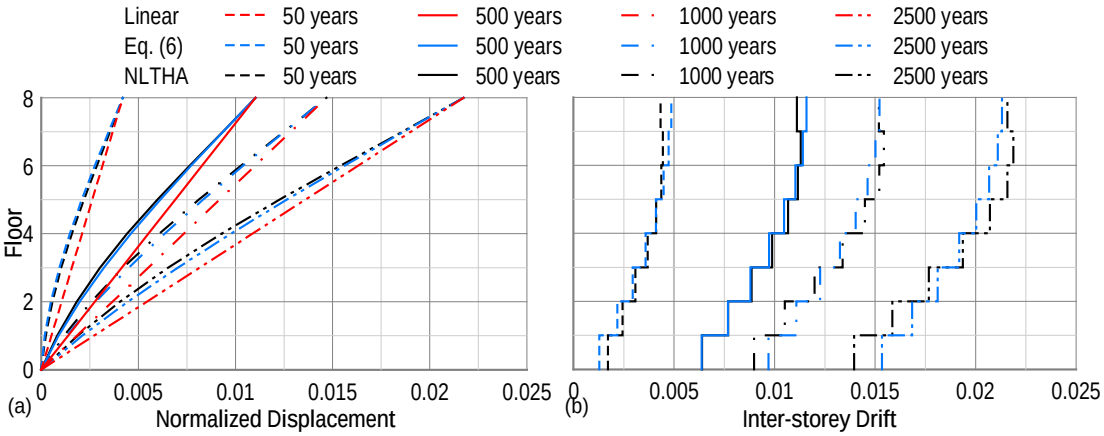

Figure 3. Case study building (a) average peak displacement and (b) inter-storey drift profiles comparison to Eq. (3).

The proposed inelastic displacement profile is given by Equation (3) and compared to different seismic intensities in Figure 3 proving more effective in fitting the numerical results.

$$\delta_i = \frac{h_i}{h_n} + \left[\frac{3}{2}\frac{h_i^2}{h_n^2}\left(1-\frac{h_i}{3h_n}\right)-\frac{h_i}{h_n}\right]\left(0.075+\frac{1}{\mu}\cdot\begin{cases}0.7 & single\,walls\\ 0.3 & coupled\,systems\end{cases}\right) \qquad (3)$$

Where h_i and h_n are the height of the i-th storey and the top storey respectively.

6 SEISMIC DESIGN COMPARISON

A few of the case study buildings was designed in accordance to NZS 1170.5 (2004) and adopting either a FBD or DBD approach providing a comparison of the two methods.

The case study buildings plan configuration shown in Figure 3 was used (similarly to the numerical analyses above) and a more comprehensive variation of the building height was accounted for (1, 2, …, 8 storeys, inter-storey height 3.6m). The buildings were designed in the Christchurch CBD (Z = 0.3), for a soil class D and a return period factor R = 1.0. The following design parameters were used: (i) ductility factor μ = 2.5; (ii) storey mass W_i = 300t; (iii) re-centering ratio β = 0.70.

The design base shear was considered as a comparison parameter for the analysis results and the resulting values are summarized in Table 2.

Displacement-Based Design resulted in smaller base design shear values than Force-Based Design. In particular DBD values ranged from 85% to 64% of the equivalent FBD base shear values. Figure 4 shows the plot of the different design values and the average shear reduction of 70% was observed (highlighted in the red dashed line).

The higher values resulting from FBD can be justified by the over-estimation of the natural period of the structure, which was chosen in accordance to empirical equations of NZS1170.5 (2004).

Table 2. Seismic design results and comparison.

ID	N_{story}	Inter-Storey Height	Total height	Base Shear		$\frac{V_{DBD}}{V_{FBD}}$
				V_{FBD}	V_{DBD}	
	(-)	*(m)*	*(m)*	*(kN)*	*(kN)*	*(-)*
1	1	3.6	3.6	1580	1345	0.85
2	2	3.6	7.2	2559	1977	0.77
3	3	3.6	10.8	3290	2307	0.70
4	4	3.6	14.4	3292	2475	0.75
5	5	3.6	18	3608	2684	0.74
6	6	3.6	21.6	3907	2799	0.72
7	7	3.6	25.2	4180	2799	0.67
8	8	3.6	28.8	4431	2810	0.63

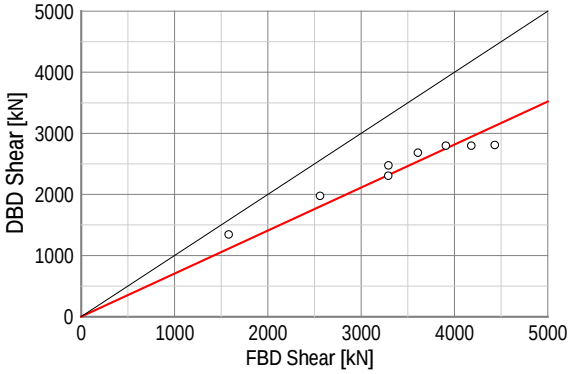

Figure 4. FBD vs DBD base shear comparison.

7 CONCLUSIONS

The paper presented suggested amendments to Force-Based and Displacement-Based Design key design parameters focusing in particular on the seismic reduction factors for both design approaches. The period estimation for FBD and the inelastic displacement profile for DBD were also discussed and amendments proposed.

Based on extensive non-linear numerical analyses carried out by the authors in accordance to the FEMA P-695 procedure (Sarti et al. 2014b), the numerical results were herein extended to the inelastic spectrum scaling factor (k_μ) which resulted to be 2.5.

The period estimation is a crucial step in the Force-Based Design of any structural system. Although classified as "other structures", empirical equation relative to concrete frames in accordance to NZS1170.5 better fitted the numerical data. The paper also provided a modification factor on the Rayleigh damping equation to account for the particular decompression behaviour of post-tensioned rocking walls.

As an alternative design approach, DBD consists in converting the structure into a single-degree-of-freedom system characterized by secant properties. In the evaluation of the seismic demand two aspects were discussed in the paper: the hysteretic viscous damping and inelastic displacement profile.

Based on static numerical analyses the authors proposed a modification factor for the current analytical formula proposed by Priestley et al. (2007) and account for particular behavioural aspects of the system.

The linear displacement profile preliminary assumed in the design phase did not reflect the observed average peak displacement profile. The paper showed a non-linear displacement profile which better fitter the numerical results.

Finally, the paper briefly discussed the outcomes of the Force-Based and Displacement-Based Design of several case study building. The results showed that DBD shear values are generally lower than FBD values. The DBD shear was in the range of 64%-85% when compared to FBD values (70% on average).

8 REFERENCES

American Society of Civil Engineers and S. E. Institute. 2010. *Minimum design loads for buildings and other structures*. American Society of Civil Engineers and S. E. Institute. Reston, (VA), American Society of Civil Engineers, Structural Engineering Institute.

Applied Technology Council for the Federal Emergency Management Agency (ATC). 2009. *Quantification of building seismic performance factors*. Applied Technology Council for the Federal Emergency Management Agency (ATC). Washington, D.C.], Washington, D.C. : U.S. Dept. of Homeland Security, FEMA.

Christopoulos, C., Filiatrault, A., Uang, C.M., Folz, B. 2002. Post-tensioned Energy Dissipating Connections for Moment Resisting Steel Frames. *Journal of Structural Engineering* 128(9): 1111-1120.

European Committee for Standardization. 2004. *Eurocode 8 - Design of structures for earthquake resistance - Part 1: General rules, seismic actions and rules for buildings*, European Committee for Standardization.

Iqbal, A., Pampanin, S., Buchanan, A.H., Palermo, A. 2007. Improved Seismic Performance of LVL Post-tensioned Walls Coupled with UFP devices. *8th Pacific Conference on Earthquake Engineering*, Singapore.

McKenna, F. 2011. OpenSees: A Framework for Earthquake Engineering Simulation. *Computing in Science and Engg.* 13(4): 58-66.

Newcombe, M. 2012. Seismic design of post-tensioned timber frame and wall buildings. *Doctor of Philosophy*, University of Canterbury.

Newcombe, M.P., Pampanin, S., Buchanan, A.H. 2010a. Design, fabrication and assembly of a two-storey post-tensioned timber building. *World Conference on Timber Engineering*.

Newcombe, M.P., Pampanin, S., Buchanan, A.H. 2010b. Global Response of a Two Storey Pres-Lam Timber Building. *New Zealand Society of Earthquake Engineering, Annual Conference.*

Newcombe, M.P., Pampanin, S., Buchanan, A.H., Palermo, A. 2008. Section Analysis and Cyclic Behavior of Post-Tensioned Jointed Ductile Connections for Multi-Story Timber Buildings. *Journal of Earthquake Engineering*.

Palermo, A., Pampanin, S., Buchanan, A.H., Newcombe, M.P. 2005. Seismic design of multi-storey buildings using laminated veneer lumber (LVL). *New Zealand Society of Earthquake Engineering, Annual Conference*, Wairakei, New Zealand, University of Canterbury. Civil Engineering.

Priestley, M.J.N. 1991. Overview of PRESSS research program. *PCI Journal* 36(4): 50-57.

Priestley, M.J.N., Calvi, G.M., Kowalsky, M.J. 2007. *Displacement-based seismic design of structures*, IUSS Press.

Priestley, M.J.N., Sritharan, S., Conley, J.R., Pampanin, S. 1999. Preliminary results and conclusions from the PRESSS five-story precast concrete test building. *Pci Journal* 44(6): 42-+.

Sarti, F., Palermo, A., Pampanin, S. 2014a. Quasi static cyclic test of 2/3 scale timber single wall and column-wall-column post-tensioned systems. *New Zealand Society for Earthquake Engineering Annual Conference*, Auckland, New Zealand.

Sarti, F., Palermo, A., Pampanin, S., Berman, J. 2014b. Evaluation of the seismic performance factors of post-tensioned timber wall systems. *2nd European Conference on Earthquake Engineering and Seismology*, Istanbul, Turkey.

Sarti, F., Smith, T., Palermo, A., Pampanin, S., Carradine, D.M. 2013. Experimental and analytical study of replaceable Buckling-Restrained Fused-type (BRF) mild steel dissipaters. *New Zealand Society for Earthquake Engineering Annual Conference*, Wellington, New Zealand.

Skinner, R.I., Kelly, J.M., Heine, A.J. 1974. Hysteretic dampers for earthquake-resistant structures. *Earthquake Engineering & Structural Dynamics* 3(3): 287-296.

Smith, T. 2014. Post-tensioned Timber Frames with Supplemental Damping Devices. *Doctor of Philosophy*, University of Canterbury.

Smith, T., Ludwig, F., Pampanin, S., Fragiacomo, M., Buchanan, A., Deam, B., Palermo, A. 2007. Seismic Response of Hybrid-LVL Coupled Walls Under Quasi-Static and Pseudo-Dynamic Testing. *NZSEE Conference.*

Spieth, H.A., Carr, A.J., Pampanin, S., Murahidy, A.G., Mander, J.B. 2004. *Modelling of Precast Prestressed Concrete Frame Structures with Rocking Beam-Column Connections.* Technical report Report 2004-01. Christchurch, New Zealand, University of Canterbury.

Standards New Zealand 2004. *AS/NZS 1170.5: Structural Design Actions - Part 5: Earthquake actions*.

Structural Timber Innovation Company. 2013. *Design Guide Australia and New Zealand- Post-Tensioned Timber Buildings*. Structural Timber Innovation Company. Christchurch, New Zealand, Structural Timber Innovation Company (STIC).